Ceramics-Silikáty 60 (3), 188-194 (2016)
journal webpage: www.ceramics-silikaty.cz doi: 10.13168/cs.2016.0028

EFFECTS OF INCORPORATING NATURAL MINERALS ON PRODUCTION AND BIOACTIVITY OF BIOACTIVE GLASS CERAMICS

#FRANCO MATÍAS STÁBILE, CRISTINA VOLZONE

Centro de Tecnología de Recursos Minerales y Cerámica (CETMIC), CONICET CCT La Plata-CICPBA. Camino Centenario y 506, M.B. Gonnet, C.P.1897, Provincia de Buenos Aires, Argentina

#E-mail: mstabile@cetmic.unlp.edu.ar

Submitted September 28, 2015; accepted April 14, 2016

Keywords: Raw materials, Glass ceramics, Bioactivity

Two glass-ceramics composition were produced from natural minerals. Quartzes and feldspars were pre-selected on the basis of their purities studied by X-ray diffraction (XRD) and chemical analysis. Prepared compositions of glasses precursors were two different theoretical leucite ($KAlSi_2O_6$)/Bioglass 45S5 (L/Bg) ratios. Transformations of raw materials mixtures and glass precursors were studied by differential thermal analyses. On the basis of thermal analysis results, glass ceramics were produced and characterized by XRD. Glass-ceramics were composed of two major crystalline phases, leucite and sodium calcium silicate. Bioactivity tests were performed submerging the glass-ceramics into simulated body fluid (SBF) for different periods (1, 5 and 10 days). Bioactive behavior was monitored by XRD and scanning electron microscopy (SEM). Studied samples were found to be bioactive, in which hydroxyapatite layer was developed within 5 days of contact with SBF.

INTRODUCTION

Taking into account that biomaterials are produced from high purity reagents, the incorporation of natural raw materials requires a special care, due to medical applications. Then, such material should have the highest possible purity, or must contain a minimum amount of undesirable components [1]. Quartz and feldspar are two of the most important components that constitute the mixture for the manufacture of glass, in addition to others like calcium and sodium carbonates, finning agents, etc. Quartz is the major component in the manufacture of glass. Feldspar ($K_2O{\cdot}Al_2O_3{\cdot}6SiO_2$) is used to incorporate alkaline oxides such as K_2O which act as a fluxing agent, and to incorporate Al_2O_3 to improve mechanical strength and chemical resistance. However, chemical resistance must be controlled in bioactive ceramics. A high chemical durability turns the material to inert. This is why the addition of Al_2O_3 into composition must be done with care, without exceeding 3 wt. % in vitreous materials [2]. But, if Al_2O_3 is incorporated within a crystalline phase in glass ceramics production, it does not interfere with bioactivity [3-5]. Both of these minerals often have Fe_2O_3 and TiO_2 impurities, which can impart color to the final product. Raw materials must be incorporated into an appropriate particle size to not extend in excess the fusion time.

Bioglass 45S5 is the most well-known and used bioactive glass, and it is the one that faster bonds to bone tissue [6]. However, its low mechanical resistance makes it not applicable in the repair of bones that can withstand load. One way to increase its mechanical strength is through crystallization, transforming it into a glass-ceramic, which does not affect its bioactivity [7], and incorporating biocompatible phases such as leucite, that is widely used in dental glass-ceramic as a reinforcement phase. It was found that leucite does not influence in glass ceramics bioactivity [5]. This work was intended to study the effect of the use of natural raw materials at all stages of production of glass-ceramics.

EXPERIMENTAL

Two quartzes and two feldspars, provided by an Argentine mining company, were characterized in order to make a pre-selection on the basis of his purity, for incorporate them into the formulation of the glasses.

Mineral particle size distributions were obtained using a Malvern Mastersizer 2000, with dispersion unit Hydro 2000 G and water as dispersant.

Raw materials used to prepare the vitrifiable mixture were reagent grade sodium carbonate, calcium carbonate, potassium carbonate, monobasic ammonium phosphate, and pre-selected natural potassium feldspar and quartz. The nominal compositions of glasses were calculated in such a way to have different theoretical weight ratios of leucite ($KAlSi_2O_6$) and Bioglass 45S5 (45 % SiO_2, 24.5 % Cao, 24.5 % Na_2O, 6 % P_2O_5). Thus there were two compositions, L25Bg75 glasses (25 wt.% leucite and 75 wt. % Bioglass) and L30Bg70 (30 wt.% leucite and 70 wt.% Bioglass).

In this way, the highest theoretical leucite content in the composition is directly related with greater feldspar aggregate.

Mixtures were fused at 1350°C for 1 hour in platinum crucible and cast on water to make glass frits. The obtained glass were milled and sieved through 400 mesh. Chemical analyses of raw materials were obtained by X-ray fluorescence in a Shimadzu EDX 800 HS equipment.

Differential thermal – thermo gravimetric analyses (DTA-TG) were conducted on a Netzsch STA409 equipment at 10°C min^{-1} in air flow of 50 $cm^3 \cdot min^{-1}$ with α-Al_2O_3 as reference substance.

X-ray diffractograms of natural raw materials, glasses and glass-ceramics were obtained by a Philips 3010 X ray diffractometer using Cu Kα radiation (λ = 1.5405 Å) at 40 kV and 20 mA and Ni filter, with 0.04° (2θ) step and 2 seconds per step.

Glass-ceramics disks were produced by heat treatment of glass powders pressed up to 110 MPa. Heat treatments were performed at 925°C for 1 hour with a heating rate of 5°C per minute. They were assessed in simulated body fluid (SBF) for 1, 5 and 10 days. The solid/solution ratio was 0.1 cm^{-1}. The solution was renewed every 5 days. Simulated body fluid was prepared following the recipe given by Kokubo et al [8].

RESULTS AND DISCUSSION

Natural minerals characterization

X-ray diffraction and chemical analysis

Figures 1a and 1b, and figures 2a and 2b, show quartzes A and B, and feldspars A and B diffractograms, respectively.

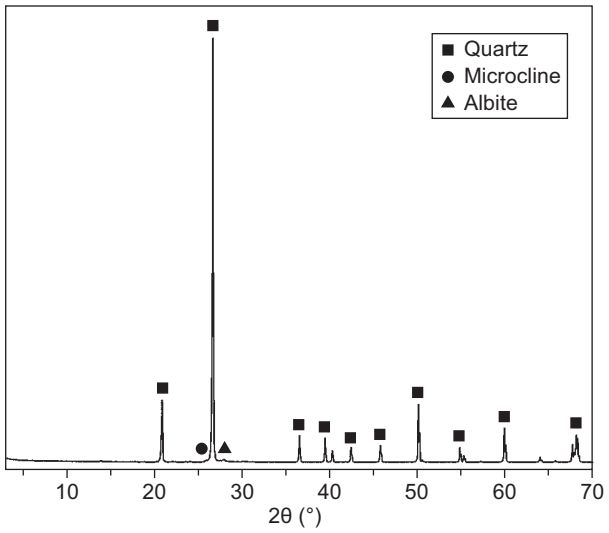

Figure 1a. Quartz A diffractogram.

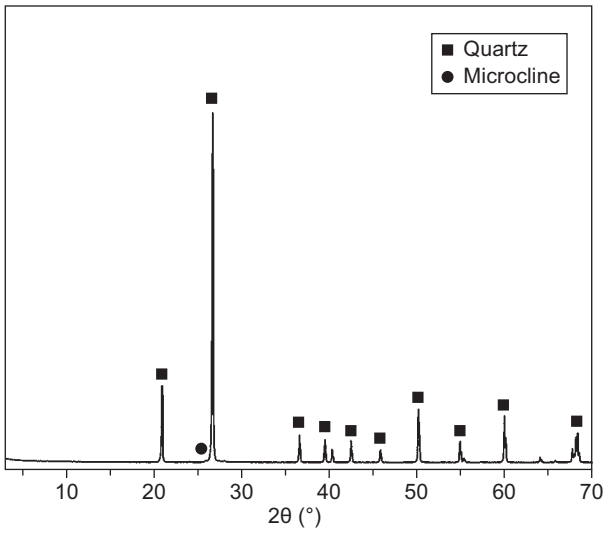

Figure 1b. Quartz B diffractogram.

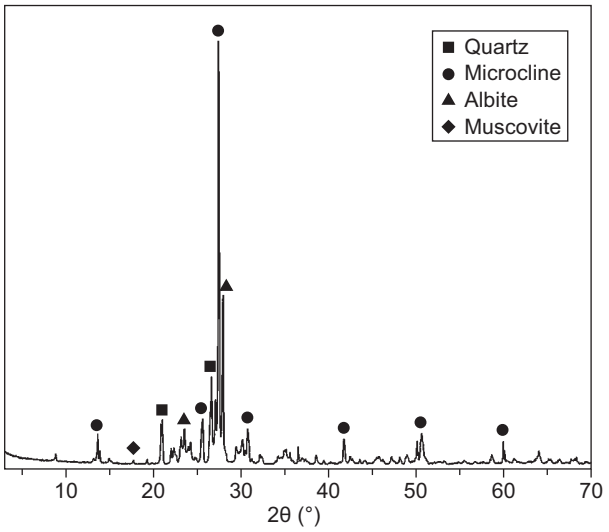

Figure 2a. Feldspar A diffractogram.

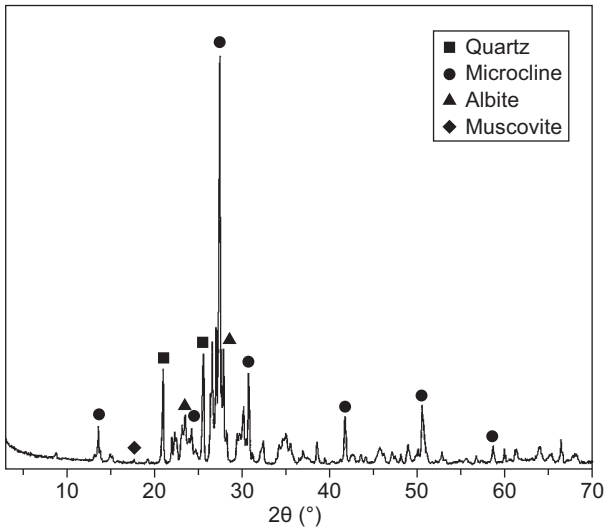

Figure 2b. Feldspar B diffractogram.

Table 1. Chemical analyses of minerals.

Raw material	SiO_2	Al_2O_3	Na_2O	K_2O	CaO	Fe_2O_3	TiO_2
Quartz A	99.33	0.49	0.06	0.10	–	0.01	0.00
Quartz B	99.49	0.36	–	0.11	–	0.03	0.01
Feldspar A	67.53	16.31	3.08	11.46	0.29	0.07	0.02
Feldspar B	66.25	18.42	2.06	12.02	0.20	0.05	0.01

Figures 1a and 1b show the presence of characteristic peaks of quartz can be seen. Quartz A is accompanied with very low amounts of albite and microcline. The chemical analysis (Table 1) showed presence of sodium and potassium oxides, which would come to be part of albite and microcline, detected by X-ray diffraction. A small peak of microcline was found in quartz B, which corresponds with the small amount of potassium measured by chemical analysis.

Figures 2a and 2b show that both feldspars are majorly composed of microcline and albite. Feldspar A has more intense albite peaks, which is consistence with a greater amount of sodium oxide detected by chemical analysis. Quartz and muscovite were also present. Quartz peaks were more intense in feldspar A.

Particle size analysis

Table 2 shows the cumulative particle size distribution data.

Table 2. Cumulative particle size distribution.

Raw material	d(0.1) (μm)	d(0.5) (μm)	d(0.9) (μm)
Quartz A	7.8	29.5	80.8
Quartz B	6.3	29.1	81.0
Feldspar A	2.1	6.2	31.7
Feldspar B	1.8	5.5	31.4

Particle sizes of quartzes and feldspars are smaller than those required in the glass industry. In general a particle size between 20 and 40 mesh is prompted (between 841 and 420 μm), since the fines are associated with impurities coming from the material used for crushing and grinding [9]. Tested raw materials have a pretreatment with permanent magnet to trap attached iron impurities, and grinding is performed by means of high alumina ball mills, which prevents pollution.

Differential thermal–thermo gravimetric analysis

Two DTA-TGs were conducted for both feldspars (Figures 3 and 4). Feldspar A does not record any mass change throughout the studied temperature range. Instead feldspar B has a single initial mass loss of around 2.5 wt. % up to 100°C. This lost is coincident with an endothermic DTA peak, which corresponds to the evaporation of free water. Feldspar A DTA curve does not denotes any appreciable transformation up to 1130°C, where a rapid signal drop is evident. In the case of feldspar B, this fall is produced from 1050°C. This temperature corresponds to feldspar softening point, which is taken into account to assess its quality [1].

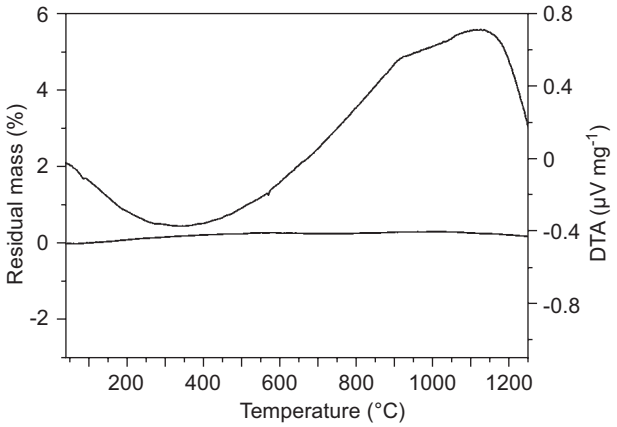

Figure 3. Differential thermal-thermo gravimetric analysis of feldspar A.

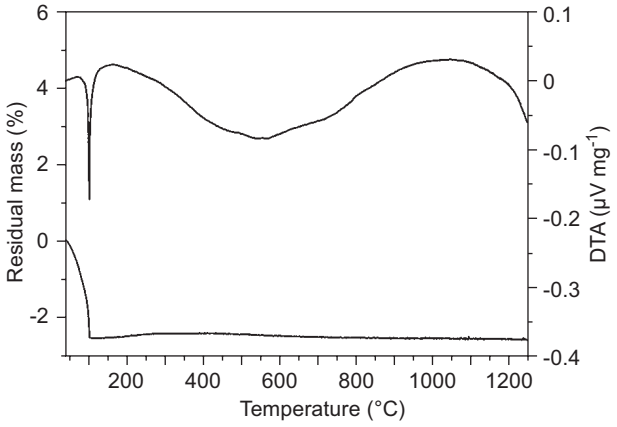

Figure 4. Differential thermal-thermo gravimetric analysis of feldspar B.

After the previous analysis, quartz A and feldspar B were selected, the first having the least amount of coloring agents, and the second the higher content of potassium feldspar, lower content of Fe_2O_3 and lower softening temperature, which is beneficial for glasses production.

Glass and glass-ceramics characterization

Differential thermal analysis

Differential thermal-thermogravimetric analysis of the vitrifiable mixtures of L25Bg75 and L30Bg70 compositions are shown in Figure 5.

Two transformations with endothermic effect can be seen between and a small mass loss 100 and 150°C in the L25Bg75 mixture. These changes correspond

to an initial decomposition of monobasic ammonium phosphate in a small amount of ammonia and phosphoric acid [10]. A well pronounced endothermic peak accompanied by a mass loss at around 200°C is observed that corresponds to the total decomposition of monobasic ammonium phosphate. This decomposition is shifted to lower temperatures in the case of L25Bg75 mixture. Carbonates transformations into their respective oxides begin close to 650°C. Then, decarbonations are completed at temperatures near 900°C. These changes become evident through the endothermic peaks in this temperature range, which are also accompanied with considerable mass losses. A difference in endothermic peaks temperatures can be seen, where that corresponding to L25Bg75 are placed at lower temperatures. An endothermic peak appears at around 1000°C, without mass change, which corresponds to the temperature at which the mixture begins to melt. The melting temperature of L30Bg70 mixture is lower than that of L25Bg75 mixture, which can be distinguished due to the higher feldspar content, which produces a greater amount of liquid, which accelerates melting.

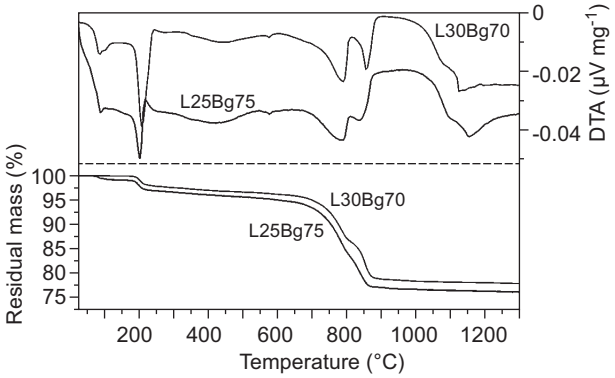

Figure 5. DTA-TG of L25Bg75 and L30Bg70 mixtures.

Figure 6 shows the differential thermal analyses of L25Bg75 and L30Bg70 glasses. Only the temperature range where the more relevant changes can be appreciated is seen. Two exothermic peak for both samples are found between 450 and 700°C. The peaks positions does not differ between both samples. The first corresponds to glass transition temperature. The second peak could not match some sort of transformation; however it will be addressed in more detail study in future work.

Between 700 and 950°C, there is a more pronounced exothermic peak, which corresponds to the crystallization of glasses. Around 750 - 775°C, a shoulder appear, indicating overlapping of two crystallization peaks, which would correspond to the formation of two major crystalline phases. The crystallization peak in L30Bg70 is located between 725 and 975°C, with a shoulder close to 775°C, so all the crystallization was shifted to higher temperatures with respect to L25Bg75. The first phase that crystallizes would be in a lower proportion than the second, since the second exothermic effect is larger. The crystallization temperatures maxima are similar. A thermal treatment temperature was selected based on the found phenomena, so as to produce ceramic pills to evaluate the degree of bioactivity. Treatment was set at 950°C for 1 hour.

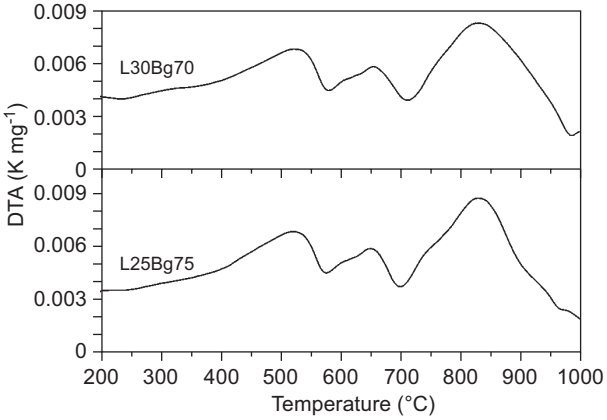

Figure 6. DTA of L25Bg75 and L30 Bg70 glasses.

X-ray diffraction

The glasses x-ray patterns can be seen at the bottom of Figure 7. A band appear centered around the 30° (2θ) (silicate), characteristic of materials that lack of long-range order. Above in the figure are shown the X-ray patterns of both heat-treated glasses, where leucite and sodium calcium silicate could be identified. It is known that leucite glass-ceramics are produced by surface crystallization mechanisms [11]. Leucite crystallization was possible to achieve for the fine glass particle size precursor, which favored surface crystallization [12].

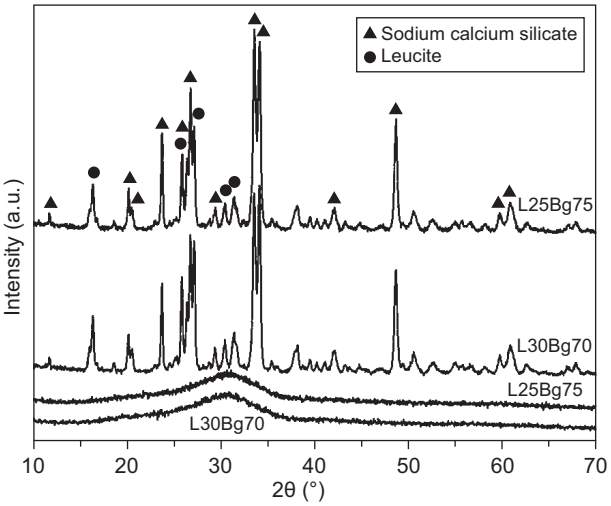

Figure 7. Glasses diffractograms with and without thermal treatment.

Leucite is in a smaller proportion than sodium calcium silicate. Relating this fact with the thermal analysis observed behaviour, it could be said that leucite is the first phase to crystallize, followed by sodium and calcium silicate crystallization. Sodium calcium silicate relative intensities decrease, while those of the leucite increase. This is in accordance with the composition change from 25 wt. % leucite and 75 wt. % Bioglass to 30 wt. % leucite and 70 wt. % Bioglass.

Leucite crystallization was possible thanks to the thermal processing of glass in powder form, since such phase in known to undergo surface crystallization that is activated with the grinding of glass [13].

Bioactivity test

X-ray diffraction

Figure 8 shows the x-ray diffractograms of L25Bg75 and L30Bg70 glass ceramics disks surfaces before and after contact with SBF for different periods of time. It may be noted that the present phases are the same after 1 day of immersion in both ceramic, although the intensities of the silicate phase decreased with respect to leucite. This is more noteworthy in L25Bg75. By increasing reaction time, a decrease in the diffraction peaks intensity is observed, resulting in hydroxyapatite formation, the most appreciable phenomenon being in L25Bg75. Hydroxyapatite appears after 5 days of immersion in L25Bg75.

As to L30Bg70, hydroxyapatite is notable after 10 days of immersion, although a good crystallinity of the formed layer was not appreciated, in opposition to what happens in L25Bg75 for the same period of time, where the peaks of the HAp have attained greater intensity and also show a higher degree of crystallinity. However, apatite formation in SBF is known to have fine crystal size, which produce diffraction peaks broadening [14, 15].

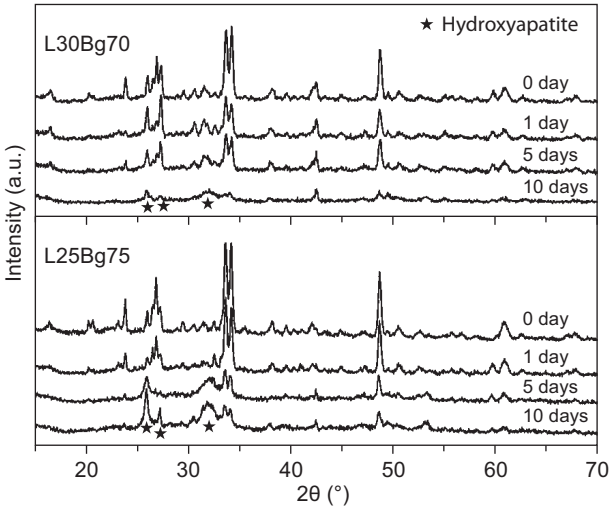

Figure 8. L25Bg75 and L30Bg70 glass-ceramics pills diffractograms unreacted and contacted with SBF for 1, 5 and 10 days.

Scanning electron microscopy

Scanning electron microscope images of the surfaces of glass-ceramics disks before and after assessment in simulated body fluid at different times are displayed in Figure 9. It was not possible to detect a surface layer presence after 1 day of contact, as well as noted by XRD.

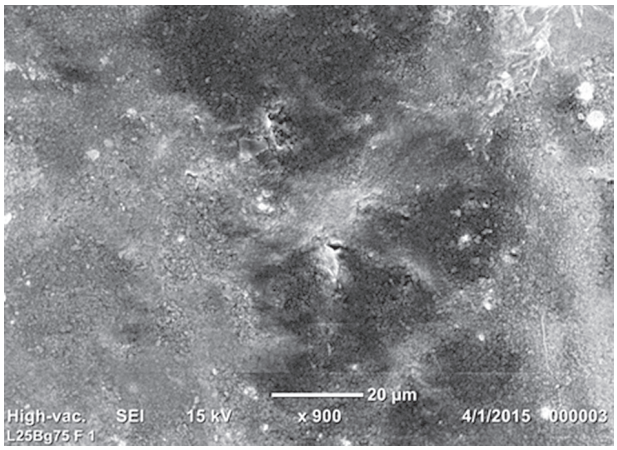

a) 1 day

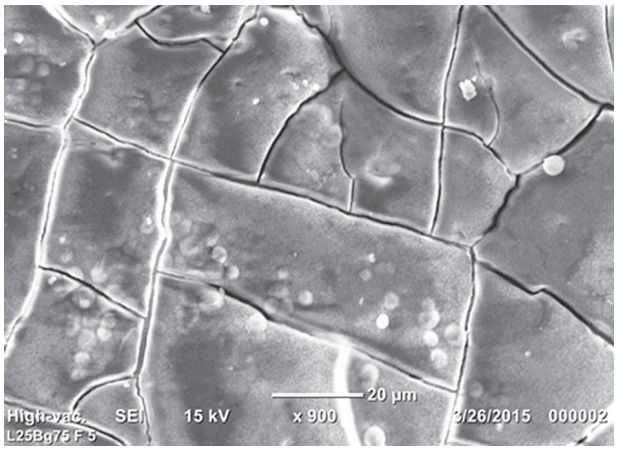

b) 5 days

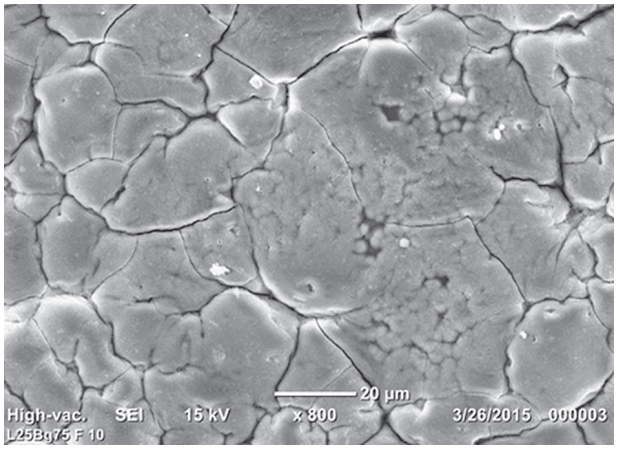

c) 10 days

Figure 9. Scanning electron microscopy of glass-ceramics after SBF immersion for different periods of time – L25Bg75.

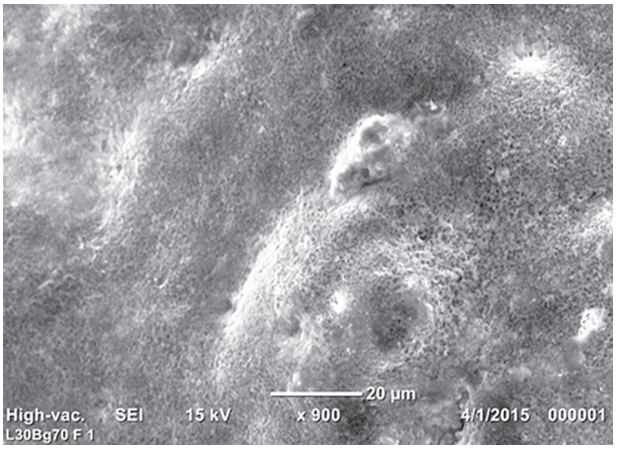

d) 1 day

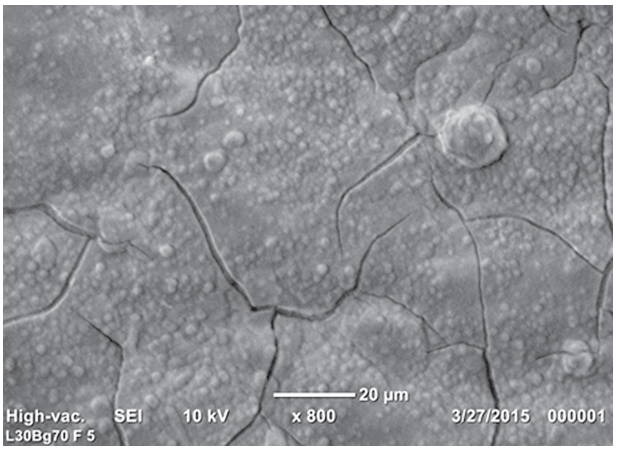

e) 5 days

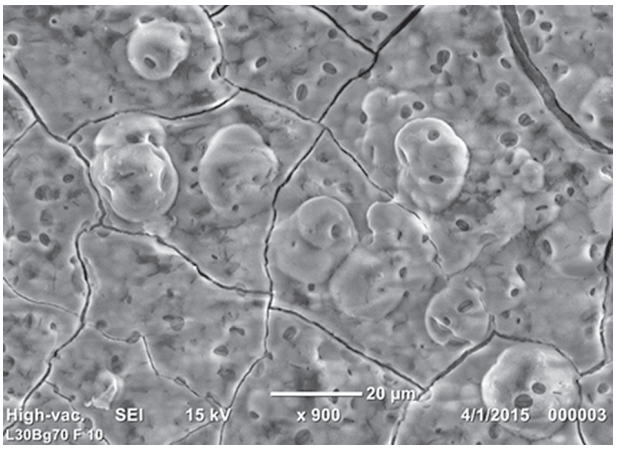

f) 10 days

Figure 9. Scanning electron microscopy of glass-ceramics after SBF immersion for different periods of time – L30Bg70.

After the 5th day of contact, it was possible to observe the formation of hydroxyapatite in both samples. The layers have cracks, which are developed after hydroxyapatite layer drying. These cracks make note that the thickness of the layer in the sample L25Bg75 was greater than that of L30Bg70. This is coincident with XRD patterns, where an increased diffraction intensity of HAp (Figure 8) was detected in the analysis of sample L25Bg75 after 5 days of immersion. Apatite layer was fully developed after 10 days of contact with SBF, as detected in the XRD analysis. A difference in the layer texture was seen, where L25Bg75 has a smooth surface while spherical agglomerates can be observed in L30Bg70.

CONCLUSIONS

Raw materials characterization by X-ray diffraction, chemical analysis and thermal analysis made it possible to choose the adequate quartz and feldspar from the standpoint of purity and fusibility, for the production of the glasses as precursor of glass-ceramics.

Thermal analyses of mixtures showed a similar behavior, although it was found that L30Bg70 (30 % Leucite, 70 % Bioglass 45S5) to produce glass had a lower fusion temperature, due to a higher feldspar content, which favors fusibility in glass production. Thermal analysis of glasses allowed determining the temperature at which the crystallization is assurance and also obtaining densified pills, so as to produce glass-ceramics containing leucite and sodium calcium silicate. It could be demonstrated through bioactivity test that the developed materials were bioactive. Sample with smaller leucite content (25 % Leucite, 75 % Bioglass 45S5) was the one that showed a higher level of bioactivity, in which hydroxyapatite could be detected by XRD and electron microscopy due to a greater developed amount. This study allows demonstrating that the obtained glass-ceramics from high purity natural minerals can be used in the production of bioactive materials. By controlling glasses precursor composition, glass-ceramics materials with different degrees of bioactivity can be obtained. In addition, if the aluminum added is controlled in such a manner as when glass glass crystallization occur, Al_2O_3 will be incorporated with a crystalline phase as leucite, it will we be able to ensure that this addition does not adversely influence the bioactivity, as if Al_2O_3 was part of the residual vitreous phase.

Acknowledgement

The authors thank to CONICET (National Council of Scientific and Technical Research) for its financial support (PIP 0248) and Jose Ortiga for his important technical assistance.

REFERENCES

1. El-Meliegy E., van Noort R. (2011). *Glasses and Glass Ceramics for Medical Applications*. Springer science & business media.
2. Hench L.L. (1991): Bioceramics: from concept to clinic. *Journal of the American Ceramic Society*, *74*(7), 1487-1510. doi:10.1111/j.1151-2916.1991.tb07132.x

3. Liu Y., Sheng X., Dan X., Xiang Q. (2006): Preparation of mica/apatite glass-ceramics biomaterials. *Materials Science and Engineering: C*, *26*(8), 1390-1394. doi:10.1016/j.msec.2005.08.017
4. Xiang Q., Liu Y., Sheng X., Dan X. (2007): Preparation of mica-based glass-ceramics with needle-like fluorapatite. *Dental Materials*, *23*(2), 251-258. doi:10.1016/j.dental.2006.10.008
5. Stábile F. M., Volzone C. (2014): Bioactivity of leucite containing glass-ceramics using natural raw materials. *Materials Research*, *17*(4), 1031-1038. doi:10.1590/1516-1439.267014
6. Lefebvre L., Chevalier J., Gremillard L., Zenati R., Thollet G., Bernache-Assolant D., Govin A. (2007): Structural transformations of bioactive glass 45S5 with thermal treatments. *Acta Materialia*, *55*(10), 3305-3313. doi:10.1016/j.actamat.2007.01.029
7. Peitl O., Dutra Zanotto E., Hench L.L. (2001): Highly bioactive P_2O_5–Na_2O–CaO–SiO_2 glass-ceramics. *Journal of Non-Crystalline Solids*, *292*(1), 115-126. doi:10.1016/S0022-3093(01)00822-5
8. Oyane A., Kim H.M., Furuya T., Kokubo T., Miyazaki T., Nakamura T. (2003). Preparation and assessment of revised simulated body fluids. *Journal of Biomedical Materials Research Part A*, *65*(2), 188-195. doi:10.1002/jbm.a.10482
9. Sinton C. W. (2006). *Raw materials for glass and ceramics: sources, processes, and quality control.* John Wiley & Sons Inc.
10. Moeller T. (1959): Phosphorus and its Compounds. Volume I: Chemistry. *Journal of the American Chemical Society*, *81*(11), 2916-2916. doi:10.1021/ja01520a086
11. Höland W., Rheinberger V., Schweiger M. (2003): Control of nucleation in glass ceramics. *Philosophical Transactions of the Royal Society of London A: Mathematical, Physical and Engineering Sciences*, *361*(1804), 575-589. doi:10.1098/rsta.2002.1152
12. Cattell M.J., Chadwick T.C., Knowles J.C., Clarke R.L., Samarawickrama D.Y. (2006). The nucleation and crystallization of fine grained leucite glass-ceramics for dental applications. *Dental Materials*, *22*(10), 925-933. doi:10.1016/j.dental.2005.10.003
13. Holand W., Beall G.H. (2012). *Glass ceramic technology*. John Wiley & Sons.
14. O'Donnell M D., Watts S.J., Hill R.G., Law R.V. (2009): The effect of phosphate content on the bioactivity of soda-lime-phosphosilicate glasses. *Journal of Materials Science: Materials in Medicine*, *20*(8), 1611-1618. doi:10.1007/s10856-009-3732-2
15. Brauer D.S., Karpukhina N., O'Donnell M.D., Law R.V., Hill R.G. (2010): Fluoride-containing bioactive glasses: effect of glass design and structure on degradation, pH and apatite formation in simulated body fluid. *Acta Biomaterialia*, *6*(8), 3275-3282. doi:10.1016/j.actbio.2010.01.043